# Session PS5.0/ST6.1
# Paper: EGU2011-214

# Distribution of currents and convection in the ionospheres of Venus and Mars

Kireev A. P. and A.M. Krymskii,

**Southern Federal University, Rostov-on-Don, RUSSIA**

## 1. Introduction

Orbit of both Mars Express and Venus Express did not allow particle and magnetic field measurements in the depth of planetary ionosphere at Mars and Venus respectively. Investigating whether or not plasma convection and distribution of currents within the ionospheres at Venus and in the northern hemisphere of Mars we utilize Pioneer-Venus Orbiter (PVO) and Mars Global Surveyor (MGS) data.

At PVO , the velocity of vertical convection of the ionospheric plasma was not measured in situ either. However, the pattern of plasma convection could be, to some extent, recovered from the magnetic field measurements by employing either theoretical or numerical models.

When PVO was able to penetrate down and below the ionization peak on the day-side of Venus the magnetic fields were usually weak throughout the day-time ionosphere of Venus. The exceptions are a) the large-scale quasi-horizontal magnetic fields which existed during (or shortly) after the "overpressure" periods (the "overpressure" means that the solar wind (SW) dynamic pressure exceeded the peak thermal pressure in the ionosphere), and b) the small-scale helical magnetic fields –the flux ropes- which were usually observed during periods of low to moderate SW dynamic pressure [Luhmann and Cravens, 1991]. In the bottom-side ionosphere, a local enhancement of the IMF strength ("magnetic belt") can exist. The occurrence rate of the either large-scale or small-scale (flux ropes) IMF inside the ionospheric plasma decreases when the SZA increases [Luhmann, 1987].

Luhmann et al [1987] suggested that the "overpressure" regime of the SW interaction with Venus would be Mars-like.

At Mars the magnetic field measurements by MAG/ER onboard MGS have shown that the localized crustal magnetic fields can form mini-magnetospheres [Connerney et al, 1999, 2001]. Outside of these mini-magnetospheres the SW and IMF can penetrate inside the Martian ionosphere. In the northern hemisphere of Mars, the crustal magnetic fields are relatively weak [Acuna et al, 1999]. Thus, a similarity between Venus and the northern hemisphere of Mars is possible.

## 2. Theoretical grounds

Within the ionospheres of Venus and Mars the inertia of electrons is negligible and the electron bulk velocity $\vec{w}_e$ satisfies the relation:

$$\vec{w}_e = \vec{W}_E + \frac{c\left[\vec{B} \times \vec{R}_e\right]}{enB^2} + w_{eb}\frac{\vec{B}}{B} \qquad (1)$$

where

$\vec{W}_E = c\frac{\left[(\vec{E} + \frac{\nabla P_e}{en}) \times \vec{B}\right]}{B^2}$ is the magnetic field convection velocity as it follows from the balance equation of magnetic field energy

$$\left(\frac{\partial}{\partial t} + \left(\vec{W}_E \cdot \nabla\right)\right)\frac{B^2}{8\pi} + \frac{B^2}{4\pi} div\left(\vec{W}_E\right) + \frac{1}{4\pi}\left(\vec{W}_E \cdot \left(\vec{B} \cdot \nabla\right)\vec{B}\right) =$$
$$- \frac{\left(\vec{B} \cdot \vec{R}_e\right)}{enB^2}\left(\vec{B} \cdot \vec{j}\right) + \frac{c}{4\pi en}\left(\vec{B} \cdot \left[\nabla n \times \nabla\left(\frac{P_e}{n}\right)\right]\right) \qquad (2)$$

Next, n is the electron density, $\vec{R}_e$ is the drag force due to electron collisions with ions and neutrals, $P_e$ is the electron pressure, $\vec{j}$ is the electric current density.

Comparison of numerically simualted and statistically established vertical profiles of the large-scale magnetic fields allows recovery of the ionosphere convection pattern within the subsolar ionosphere of Venus and Mars where bulk velocities of ionospheric plasma components are too small to be accurately derived from particle mesurements data.

$\vec{j}$ can also be evaluated from the statistically established vertical profiles of the large-scale magnetic fields:

$$\vec{j} = \frac{c}{4\pi} curl\vec{B}$$

## 3. Experimental data

### 3.1 Venus

On the day-side of Venus, at the altitudes less than 200 km, the IMF is transported downward by a descending flow of ionospheric plasma [Phillips et al, 1984].

In 1-D case, the magnetic field strength B and the velocity of the descending flow $v_z$ satisfy approximately the condition for the stationary downward convection [ Phillips et al, 1984]:

$$v_z B \approx v_{z0} B_0 > 0 \qquad (3)$$

$v_z(z_0) = v_{z0}$ and $B(z_0)=B_0$. B decreases when $v_z$ increases and vice versa.

Next, the electron density n and $v_z$ approximately satisfy the stationary particle balance equation:

$$\frac{d}{dz}(n v_z) \approx -J_{CO_2} N_{CO_2} + k_1 n^2 . \qquad (4)$$

Here, z is the altitude, $N_{CO_2}$ is the carbon dioxide density, $J_{CO_2}$ is the photo ionization rate of carbon dioxide, $k_1$ is the recombination rate of molecular ions $O_2^+$.

The derivative of the velocity of the descending flow $dv_Z/dz$ satisfies the relation:

$$\frac{dv_z}{dz} \approx \frac{1}{n}[v_z \frac{dn}{dz} - (J_{CO_2} N_{CO_2} - k_1 n^2)] \qquad (5)$$

$dv_Z/dz \approx 0$, that is $v_z$ is close to its maximum, when dn/dz and $[J_{CO_2} N_{CO_2} - k_1 n^2]$ are negligibly small. That is the maximum of $v_z$ is located near the ionization peak.

Thus local minimum of B must be near the ionization peak. This local minimum was assumed to be the top-side boundary of the “magnetic belt” at Venus.

### 3.2 Mars

#### ***<u>3.2.1 Assessment of ionization peak location in the subsolar region using MGS radio occultation data</u>***

If a) the neutral atmosphere scale-height, $H_n$, does not vary with altitude and SZA, and b) the neutral atmosphere density on the surface of Mars is independent of the latitude and longitude, then the altitude of the ionization peak $z_{peak}$ ,as a function of $\chi$, satisfies the equation:

$$z_{peak}(\chi) = z_{sub} - H_n \ln(\cos\chi) \qquad (6)$$

where $z_{sub}$ is $z_{peak}$ at the subsolar point [Kliore, 1992].

For the 732 electron density profiles obtained during the radio occultation experiment in the northern hemisphere, $z_{peak}$ as a function of SZA and $H_n$ as a function of $z_{peak}$ are presented in Figure 1.

The curve $z_{peak}(\chi) = A - B\ln(\cos\chi)$ best fits the data presented in Figure 4, if $z_{sub}$ =A = 123.8±0.6 km and $H_n$ =B = 6.4±0.3 km. $H_n$, which is derived by this method, is lower than which was observed in most of the cases (Figure 1). Next $H_n$ correlates with $z_{peak}$, and $dH/dz_{peak}$ = 0.30±0.02, on the average.

If the average values of $z_{peak}$=134,4±3.7 km and $H_n$=10.1±2.5 km, which are derived for 448 profiles at SZA from 76 to 82$^o$ where $z_{peak}$ varies insignificantly (see Figure 4), are substituted into Eq.(6), $z_{sub}$ ≈ 115 - 117 km.

Despite of substantial uncertainty in $z_{sub}$ derived from eq.(5), the estimated $z_{sub}$= 115-125 km is appropriate for qualitative analysis of IMF convection in the Martian ionosphere.

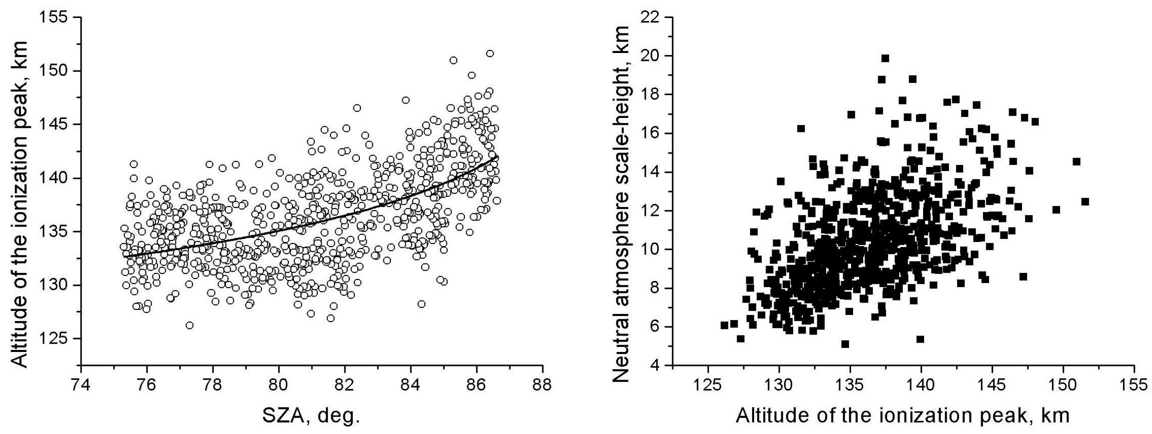


**Figure 1.** LHS panel: The altitude of the ionization peak as a function of the solar zenith angle ($\chi$) for 732 electron density profiles obtained in the northern hemisphere. Solid line indicates the best fit $z_{peak}(\chi) = A - B\ln(\cos\chi)$. RHS panel: The neutral atmosphere scale-height at the altitude of the ionization peak as a function of the ionization peak altitude for 732 electron density profiles obtained in the northern hemisphere.

## *3.2.2 Analysis of MAG/ER data*

We use the MAG/ER data collected at altitudes from 90 to 180 km at the dayside of Mars during the elliptical orbits of MGS, which are then averaged [Connerney et al, 2001].The median SW dynamic pressure at the orbit of Mars is assumed to be $10^{-8}$ dyn/cm$^2$, and the criterion is applied

$$\frac{B^2}{8\pi} < 2*0.88*\cos^2\psi \cdot 10^{-8}\, dyn/cm^2 \quad , \quad (7)$$

to eliminate sampling of the strong crustal magnetic fields [Krymskii et al, 2003]. The latitude,$\psi$, is assumed to be a proxy of $\chi$ in spite of $\psi$ can deviate from $\chi$ due to the tilt of the Martian rotation axis, the SW flow aberration, the non-spherical nominal obstacle and other considerations.

For the magnetic fields satisfying the criterion (7), we analyze histograms of the magnetic field angle with local zenith and the magnetic field pressure.

Within the latitude interval 15$^o$-30$^o$, the contribution of weak crustal magnetic fields to the altitude profile of the magnetic field pressure is minimal. We use the characteristics of the magnetic field at altitudes 170-180 km as a reference for the analysis of the vertical convection of the draped IMF.

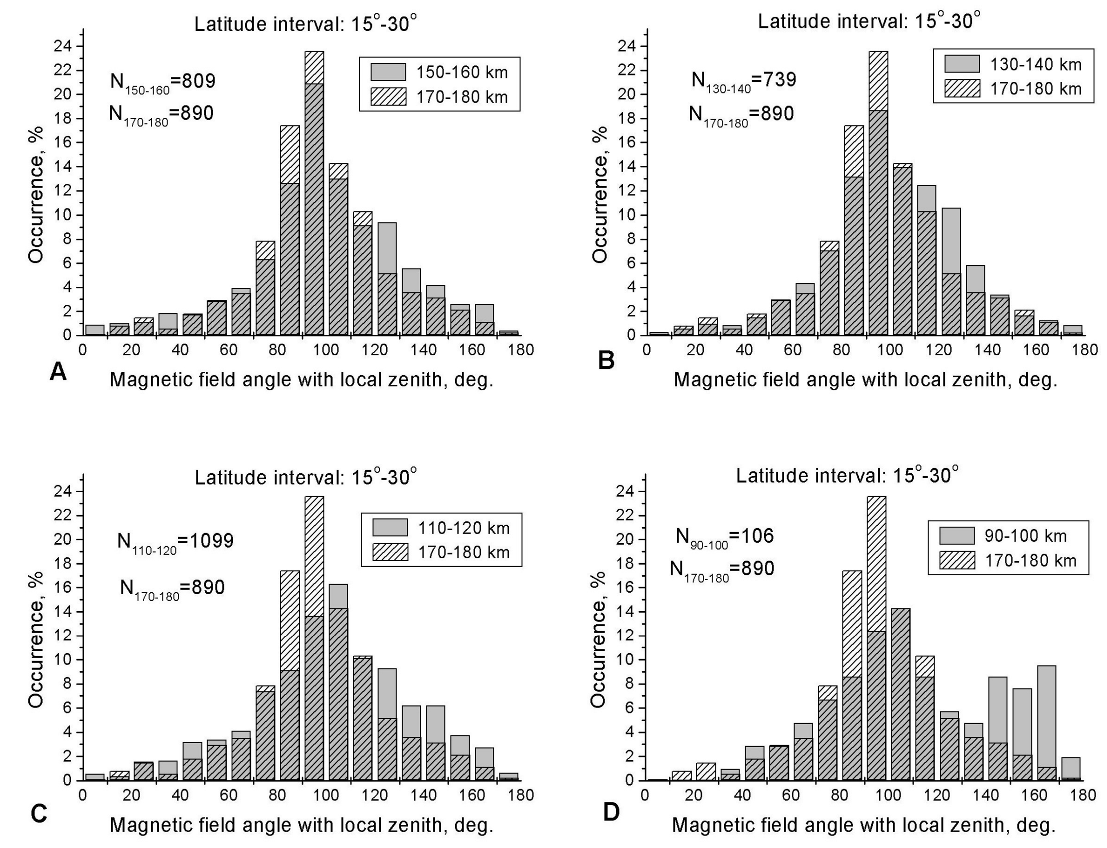


**Figure 2.** Histogram of the occurrence rate of the angle between the local zenith and magnetic fields for the latitude interval 15$^o$ -30$^o$: panel A- at 150-160 km, panel B - at 130-140 km, panel C - at 110-120 km, panel D - at 90-100 km.

In each panel the histogram of the occurrence rate of the angle between the local zenith and magnetic fields at 170-180 km for the latitude interval 15$^o$ -30$^o$ is shown as a reference.

$N_{170-180}$, $N_{150-160}$, $N_{130-140}$, $N_{110-120}$ and $N_{90-100}$ are the total number of magnetic fields analyzed in the each altitude interval, respectively.

In Fig.2, in panel D (the altitude interval 90-100 km), the histogram is noticeably different from the histogram of the draped IMF (the altitude interval 170-180 km). The angles larger than $90^o$ are much more numerous. This indicates that the vertical transport of the draped IMF is practically terminated at 100-110 km.

The percent of the strong crustal magnetic fields, which do not satisfy criterion (7), increases when the altitude decreases except for the altitudes 90-100km. This also indicates a larger effect of the crustal magnetization at lower altitudes.

The lower percent of the strong crustal magnetic fields at 90-100 km than at 110-120 km seems to be due to the crustal magnetic fields being underrepresented because of relatively low number of magnetic field measurements at altitudes of 90-100 km.

**Table 1**. Occurrence rate of of the strong crustal magnetic fields, which do not satisfy criterion (7), for latitudes $15^o$-$30^o$

| **Altitude interval** | **Total number of magnetic field measurements** | **Percent of strong crustal fields** |
|---|---|---|
| **170-180 km** | **981** | **9** |
| **150-160 km** | **940** | **14** |
| **130-140 km** | **966** | **23** |
| **110-120 km** | **1517** | **28** |
| **90-100 km** | **141** | **23** |

The occurrence rate of low magnetic field pressure increases when the altitude decreases (from panel A to panel D in Fig. 3).

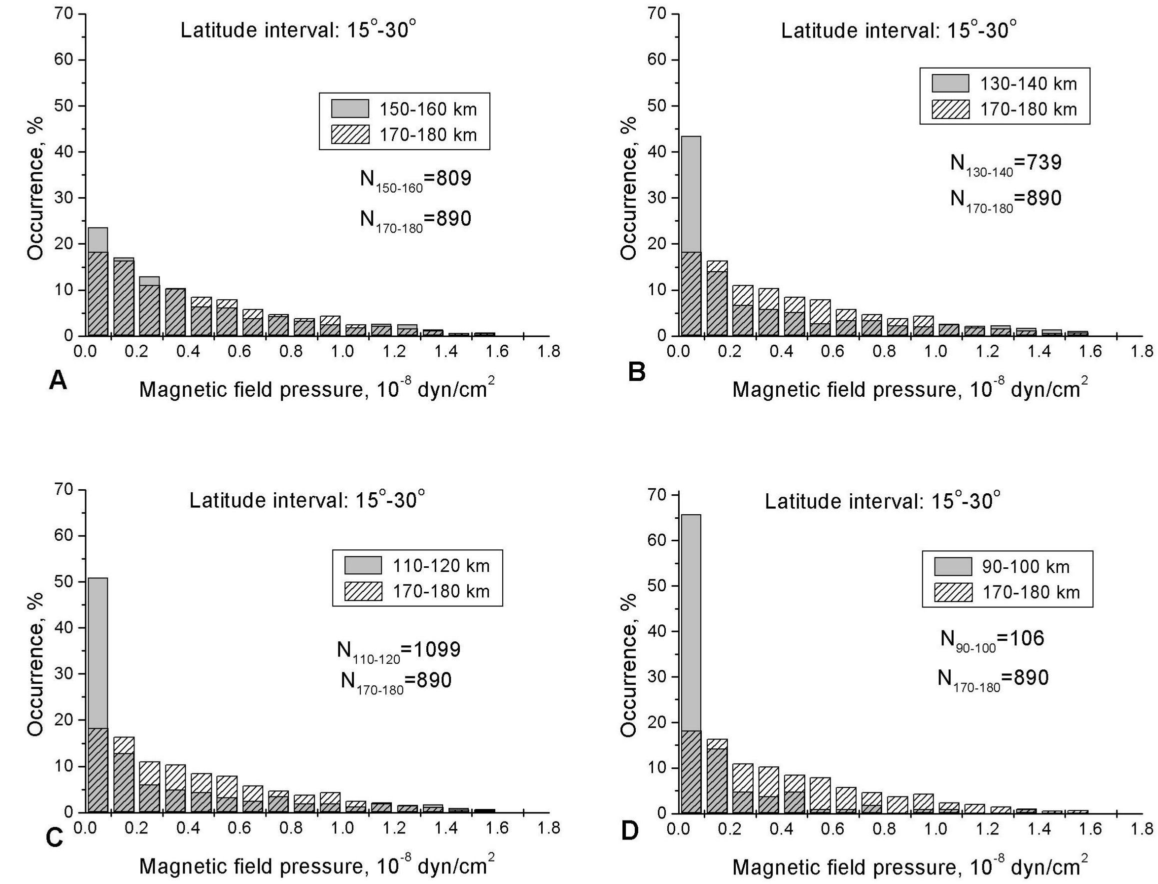


**Figure 3.** Histogram of the occurrence rate of the magnetic field pressure for the latitude interval 15° -30° : : panel A- at 150-160 km, panel B - at 130-140 km, panel C - at 110-120 km, panel D - at 90-100 km.

In each panel the histogram of the occurrence rate of the magnetic field pressure at 170-180 km for the latitude interval 15° -30° is shown as a reference.

$N_{170-180}$, $N_{150-160}$, $N_{130-140}$, $N_{110-120}$ and $N_{90-100}$ are the total number of magnetic fields analyzed in the each altitude interval, respectively.

## 4.Discussion

At Venus, during (or shortly after) “overpressure” periods, the local enhancement of the strength of the large-scale IMF – magnetic belt - indicates that : a) the ion-neutral collisions substantially decelerate the descending flow of the ionospheric plasma below the ionization peak and b) the IMF convection is approximately 1-D.

At Mars within the latitude interval of $15^o$-$30^o$ and at altitudes higher than 110 km, the altitude profile of the IMF pressure agrees with the results of the numerical simulations in Shinagawa and Bougher [1999]. No “magnetic belt” has been observed in their computations either. To extend the numerical simulations to lower altitudes the crustal magnetization must be properly included in the model.

In the northern hemisphere at Mars, which is belived to be Venus-like, the Martian crustal magnetization primarily determines the magnetic fields at altitudes less than 110 km. Within the latitude interval $15^o$-$30^o$, the ionization peak is expected to be located at the altitude 115-125 km that is close to 100 km altitude where, as shown, the Martian crustal magnetization primarily determines the magnetic fields.

Presumably downward flux velocity significantly decreases near the ionization peak but there is no magnetic field enhancement predicted by the 1-D model of IMF downward convection. That implies that IMF convection is essentially multi-dimensional or/and nonstationary throughout the region of Martian ionopshere analyzed. In particular, in the case of 2-D model which admits a horizontal transport of IMF, one gets from Eq. (2) that

$$v_z B \approx v_{z0} B_0 - \int_z^{z_0} div\left(B\vec{W}_{Eh}\right)dz > 0 \qquad (8)$$

and deceleration of the downward flow is not always followed by the magnetic field enhancement. In Eq. (8) $\vec{W}_{Eh}$ is the horizontal component of $\vec{W}_E$ .

As shown in Breus et al (2005) the magnetic fields drive day-to-night convection near the terminator in the northern hemisphere of Mars

In the southern hemisphere, where the crustal magnetization is stronger, the crustal magnetic fields may prevent the IMF convection/diffusion at altitudes significantly higher than 110 km.

The IMF to crustal fields transition occures in a layer of 10-20 km and looks like rotational discontinuity. The small-scale helical magnetic fields can also be formed following a reconnection of the crustal magnetic fields with IMF. The strength of reconnecting fields is approximately equal. The helical magnetic fields resulting from any reconnection will not appear as a pulse of the magnetic field strength on the lower background.

## 5. Conclusions

The remnant magnetization of the Martian crust and lower density of the neutral atmosphere make the current systems and IMF/plasma convection patterns at Venus and Mars essentially different.

In particular, in contrast with Venus, at Mars a) the current layers are expected to be mainly associated with rotational dicontinueties and b) within the bottom-side ionosphere the plasma convection is essentially multi-dimensional and/or non-stationary.

## *REFERENCES:*

**Acuña, M.H., J.E.P. Connerney, N.F. Ness, R.P. Lin, D.L. Mitchell, C.W. Carlson, J. McFadden, K.A. Anderson, H. Reme, C. Mazelle, D. Vignes, P. Wasilewski, and P. Cloutier,** Global distribution of crustal magnetism discovered by the Mars Global Surveyor MAG/ER experiment, *Science, 284*, 790-793, **1999.**

**T.K. Breus, N.F. Ness , A.M. Krymskii, D.H. Crider, M.H. Acuna, J.E.P. Connerney, D. Hinson and K.K. Barashyan,** The effect of crustal magnetic fields and the pressure balance in the high latitude ionosphere/atmosphere at Mars, Adv. Space Res., doi:10.1016/j.asr.2005.01.100, **2005.**

**Connerney, J., M. Acuña, P. Wasilewski, N. Ness, H. Rème, C. Mazelle, D. Vignes, R.Lin, D. Mitchell, and P. Cloutier,** Magnetic lineations in the ancient crust of Mars, *Science, 284*, 794-798, **1999.**

**Connerney, J. E. P., M. H. Acuña, P. J. Wasilewski, G. Kletetschka, N. F. Ness, H. Rème, C. Mazelle, R. P. Lin, D. L. Mitchell,** The global magnetic field of Mars and implications for crustal evolution, *Geophys. Res. Lett., 28*, 4015-4018**, 2001.**

**Krymskii, A. M.; Breus, T. K.; Ness, N. F.; Hinson, D. P.; Bojkov, D. I.,** Effect of crustal magnetic fields on the near terminator ionosphere at Mars: Comparison of in situ magnetic field measurements with the data of radio science experiments on board Mars Global Surveyor, Journal of Geophysical Research, Volume 108, Issue A12, pp. SIA 5-1, CiteID 1431, DOI 10.1029/2002JA009662, **2003**

**Luhmann, J.G. ,** The Solar Wind Interaction with Venus, SPACE SCIENCE REVIEWS, vol. 44, 241-306, **1987**

**Luhmann, J. G.; Russell, C. T.; Scarf, F. L.; Brace, L. H.; Knudsen, W. C.** Characteristics of the Mars-like limit of the Venus-solar wind interaction, Journal of Geophysical Research, vol. 92, p. 8545-8557, **1987**,

**Luhmann, J. G.; Cravens, T. E.** Magnetic fields in the ionosphere of Venus, Space Science Reviews , 55, p. 201-274, **1991**.

**Phillips, J. L.; Luhmann, J. G.; Russell, C. T.** Growth and maintenance of large-scale magnetic fields in the dayside Venus ionosphere, Journal of Geophysical Res., 89, p. 10676-10684, **1984**

**Shinagawa, H.; Bougher, S. W.** A two-dimensional MHD model of the solar wind interaction with Mars, Earth, Planets and Space, Volume 51, p. 55-60, **1999**